



Article

Fructose-Derived Carbon Dots as Selective Antitumor Agents in Breast Cancer Therapy: Synthesis, Characterization, and Biological Evaluation

Sofia Magalhães ^{1,2}, Carla Luís ^{1,3,4,*}  and Abel Duarte ^{2,5,6,*} 

- ¹ Department of Biomedicine, Faculty of Medicine of University of Porto, Al. Prof. Hernâni Monteiro, 4200-319 Porto, Portugal
- ² Superior Institute of Engineering of Porto (ISEP), Polytechnic of Porto, Rua Dr. António Bernardino de Almeida, 4249-015 Porto, Portugal
- ³ Institute of Investigation and Innovation in Health (I3S), Rua Alfredo Allen, 208, 4200-135 Porto, Portugal
- ⁴ School of Medicine and Biomedical Sciences, Fernando Pessoa University (EMCB/UFP), Praça de 9 de Abril 349, 4249-004 Porto, Portugal
- ⁵ REQUIMTE/LAQV, ISEP, Polytechnic of Porto, Rua Dr. António Bernardino de Almeida, 4249-015 Porto, Portugal
- ⁶ Center of Innovation in Engineering and Industrial Technology, ISEP, Polytechnic of Porto, Rua Dr. António Bernardino de Almeida, 4249-015 Porto, Portugal
- * Correspondence: carlaluis@ufp.edu.pt (C.L.); ajd@isep.ipp.pt (A.D.)

Abstract: This study explored a novel method using fructose-derived carbon dots (FCDs) for anti-tumor therapy in breast cancer (BC), marking a pioneering use of fructose as a carbon source for nanoparticle synthesis. BC, known for its complexity and heterogeneity, was chosen as a model due to its increasing mortality and incidence rates. The FCD synthesis involved the decomposition of fructose through microwave irradiation, followed by purification and characterization using techniques such as transmission electron microscopy, dynamic light scattering, fluorescence spectrophotometry, and Fourier-transform infrared spectroscopy. The FCDs, ranging in size from 2 to 6 nm, presented a hydrodynamic diameter below 2 nm, a spherical morphology, and a crystalline structure. As expected, FCDs were composed by carbon, oxygen, and hydrogen, and exhibited fluorescence with absorption and emission spectra at 405 nm and around 520 nm, respectively. Cell-based assays on breast epithelial and tumor cell lines demonstrated a dose-dependent response, with a decreased viability rate more pronounced in breast tumor cells. In conclusion, FCDs showed significant potential as selective antitumor agents for breast cancer therapy. The comprehensive characterization and cell-based assay evaluations provided valuable insights into the applications of these nanoparticles in breast cancer treatment, highlighting their selective toxicity and impact on tumor cells.

Keywords: carbon dots; breast cancer; fructose; fructose-derived carbon dots; nanotechnology



Citation: Magalhães, S.; Luís, C.; Duarte, A. Fructose-Derived Carbon Dots as Selective Antitumor Agents in Breast Cancer Therapy: Synthesis, Characterization, and Biological Evaluation. *J* **2024**, *7*, 584–591. <https://doi.org/10.3390/j7040035>

Academic Editor: James David Adams

Received: 9 October 2024

Revised: 29 November 2024

Accepted: 19 December 2024

Published: 22 December 2024



Copyright: © 2024 by the authors. Licensee MDPI, Basel, Switzerland. This article is an open access article distributed under the terms and conditions of the Creative Commons Attribution (CC BY) license (<https://creativecommons.org/licenses/by/4.0/>).

1. Introduction

Carbon nanomaterials, including carbon nanotubes, carbon quantum dots (CQDs) and carbon nanoparticles, refer to nanoscale carbon-based materials. Fructose-derived carbon dots (FCDs) are classified as carbon-based nanomaterials due to their derivation from the carbohydrate precursor fructose [1]. Their characteristics include photoluminescence, good biocompatibility, and a wide range of chemical and physical properties which have been explored in drug delivery systems, bioimaging, biosensing, as well as microbial, photothermal, and photodynamic therapy [2]. Carbon dots have been the focus of academic research in recent decades, with promising results, namely in cancer diagnosis and treatment.

In cancer therapy, the effectiveness of Photodynamic Therapy (PDT) and Photothermal Therapy (PTT) can be significantly enhanced with CQDs, owing to their exceptional photoluminescence properties. While PDT uses photosensitizers to generate reactive oxygen

species, causing oxidative damage to cancer cells, PTT employs photothermal agents to convert light energy into heat, leading to localized tumor destruction [3]. Markovic and colleagues were the first to demonstrate the photodynamic cytotoxic effects of CDs on cancer cells [4]. Since then, there has been increasing interest, leading to a vast body of literature regarding research in CQD-associated phototherapies. Regarding PTT, a system that utilizes lecithin-derived self-assembled carbon dots has been described. These types of CQDs exhibit remarkable photothermal efficiency, red-shifted fluorescence, and enhanced phototoxicity against cancer cells when combined with near-infrared light exposure [5]. Another interesting study improved PDT efficacy with a CQD agent and a high singlet oxygen generation [4].

Also, CQDs are noted for their ability to stabilize, solubilize, encapsulate, and enhance targeted cancer chemotherapy. Their excellent solubility and biocompatibility enable the stabilization and solubilization of many hydrophobic chemotherapeutic agents, thereby improving their efficacy [3]. Additionally, surface modifications of CQDs allow a more precise targeting therapy to specific tumor cells. An interesting review by Bhattacharya and colleagues described and summarized diverse carbon sources, synthesis methods, nanodrug conjugations and complexation techniques in which CQDs resulted in promising outcomes in numerous types of cancer [6].

Our study focused on breast cancer (BC) due to our group's expertise and because BC is one of the most prevalent cancers, particularly among women [7]. BC is a complex and heterogeneous disease, with several clinical and pathological characterizations being the receptor status the most decisive on the patient therapeutic strategy. BC can be molecularly classified according to the status of the estrogen receptor (ER), progesterone receptor (PR) and human epidermal growth factor receptor 2 (HER2) [8] into luminal A (ER+, PR+, HER2-, Ki67+) and B (ER+, PR+, HER2+/HER2-, Ki67+), HER2-enriched (ER+, PR+, HER2+) and triple-negative (ER-, PR-, HER2-) [9]. Receptor status helps direct treatment decisions, enabling the implementation of more precise and effective therapies tailored to the specific tumor characteristics. The introduction of CQDs in the diagnosis and treatment of BC represents a promising approach that has the potential to restructure how this devastating disease is addressed, encompassing prevention, early detection, and effective treatment [10,11].

Our study aimed to develop, synthesize and characterized novel FCDs and evaluate their therapeutic potential in breast cancer. This comprehensive characterization and assessment in cell-based assays will allow for valuable insights into the potential therapeutic application of these carbon nanomaterials in breast cancer treatment.

2. Materials and Methods

2.1. FCD Synthesis

FCDs were synthesized using a previously described protocol [12] with minor alterations. In summary, 11 g of D-fructose (Panreac, Chicago, IL, USA) was added to 16 mL of deionized water and 55 mL of polyethylene glycol 200 (DEG) (Scharlau, Barcelona, Spain). From the final homogenized solution, 13 mL was allowed to react in a conventional microwave (Becken, Matosinhos, Portugal) at med-high temperature (700 W) for 5 min.

2.2. FCD Purification

Dialysis was performed using a dialysis membrane (Spectra/Per Dialysis membrane Biotech Ce Tubing MWCO: 100–500 Da) (Repligen, Waltham, MA, USA) against deionized water for 24 h to remove the organic solvent. Dialyzed FCDs were centrifuged at $21,000 \times g$ for 2 h. Afterwards, the supernatant was harnessed and filtered through a filter membrane of 0.22 μm to remove larger particles. The obtained solution was filtered on a 3 kDa MWCO centrifugal filter (Vivaspin, Littleton, MA, USA) to obtain homogeneous particles smaller than 3 kDa. The sample was frozen at $-80\text{ }^{\circ}\text{C}$ for 24 h. It was then placed in the freeze-dryer for 3 days at $-86\text{ }^{\circ}\text{C}$ and 200 mTorr. A caramel-like compound was obtained, easily handled in characterization techniques and cellular assays.

2.3. FCD Characterization

Fluorescence was measured by a fluorometer equipped with a detector USB 2000 Ocean Optics, an optic fiber connected to a cube tip QP600-2-VIS-BX-Ocean Optics (Cuv Sample Holder of 4 pathways) (Hitachi, Abingdon, United Kingdom) and an excitation LED of 405 nm. The absorbance measurement was performed in the spectrophotometer (Nanocolor-Advance, Macherey-Nagel, Dueren, Germany) using a wavelength between 360 nm and 800 nm. Hydrodynamic diameter and zeta potential were performed using a Malvern Zetasizer Nano ZS (Malvern panalytical, Malvern, UK). Measurements were performed in triplicate at 25 °C, with light detection at 273° and electrophoretic light scattering at 17°. Morphology, size, and structure were determined by transmission electron microscopy (TEM) Jeol JEM-2100-HT, 200 kV (Jeol, Freising, Germany). Fourier-transform infrared spectroscopy (FTIR) was used to characterize surface functional groups. Infrared spectrum was obtained by Nicolet 6700 FT-IR Spectrometer (Thermo Electron Corporation, Waltham, MA, USA). A parallel technique using two circular NaCl windows was executed, given the caramel consistency of the sample.

2.4. Cellular Culture

Human mammary, non-tumorigenic epithelial cell line MCF-10A (American Type Culture Collection, Manassas, VA, USA) was cultured in Dulbecco's Modified Eagle Medium (DMEM)/Ham's F-12 (GIBCO-Invitrogen, Carlsbad, CA, USA) supplemented with 100 ng/mL cholera toxin, 20 ng/mL epidermal growth factor (EGF), 0.01 mg/mL insulin, 500 ng/mL hydrocortisone, and 10% horse serum. All growth factors were purchased from Sigma (St. Louis, MO, USA) [13]. The cells were used between passages 25 to 36.

Human breast carcinoma cell line BT474 was cultured in DMEM (Sigma-Aldrich, St. Louis, MO, USA), supplemented with 20% Fetal Bovine Serum (FBS, Invitrogen Life technologies, Carlsbad, CA, USA), 1% penicillin/streptomycin (Invitrogen Life technologies, Carlsbad, CA, USA) and 3.7 g/L sodium bicarbonate (Sigma-Aldrich, St. Louis, MO, USA) and maintained at 37 °C in a humidified atmosphere containing 5% CO₂. The cells were used between passages 13 to 38. BT474 is an epithelial-like cell line characterized by expressing both hormonal and HER2 receptors [14]. Being triple positive, they can be particularly useful in research focusing on therapeutic strategies such as the use of CQDs as drug delivery systems.

Treatments were performed using respective mediums, without supplementation, with different concentrations of FCDs. No treatment was applied in the control condition. All samples were assayed in triplicates of three replicates. The mean value for each experiment was calculated. The results were given as mean ± standard deviation and are expressed as a percentage of the control, which was considered to be 100%.

2.5. Cellular Viability (MTT Assay)

MCF-10A and BT474 (1×10^5 cells/mL) were seeded in a 96-well plate and allowed to grow for 24 h. Afterwards, treatments were administered for 24 h in a serum-free medium according to previous studies in carbon dots and breast cancer cell lines [15]. A FCD concentration range of 1 to 10 mg/mL was used to assess the impact of FCD in cell behavior. The concentration range was selected based on previous studies involving the application of CQDs in breast cancer cell lines [16,17].

Cells were then subjected to MTT [3-(4,5-dimethylthiazol-2-yl)-2,5-diphenyl tetrazolium bromide] (Abcam, Cambridge, UK) at a final concentration of 0.5 mg/mL for 3 h and then lysed in DMSO (Merck, Darmstadt, Germany). The MTT assay is a colorimetric method used to evaluate cell metabolic activity. It relies on NAD(P)H-dependent cellular oxidoreductase enzymes, which reduce the tetrazolium salts in the MTT compound to a colored product, formazan (purple), thereby indicating cellular viability using spectrophotometry. Optical density was measured at 550/560 nm in a UV-VIS spectrophotometer

(MultiSkán Ascent, Thermo Fisher, Waltham, MA, USA). The background absorbance was subtracted.

2.6. Statistical Analysis

Results were expressed in mean \pm SD (Standard Deviation). Data were analyzed by one-way analysis of variance (ANOVA) using GraphPad Prism 8, and a p -value < 0.05 was considered statistically significant.

3. Results

3.1. FCD Synthesis Process

FCDs were examined for their optical attributes through UV-vis absorption and fluorescence emission spectrum assessments. As illustrated in Figure 1A,B, FCDs exhibited abundant absorption in the near-UV region and an emission spectrum with a broad band at approximately 520 nm when irradiated at 405 nm. The characteristic decline in absorption from the ultraviolet to the visible range was evident, aligning with the typical behavior of carbon dots. Following the dialysis process, a reduction in fluorescence was noted, providing confirmation of the successful removal of DEG from the FCD mixture, as depicted in Figure 1C–F. Following, FCD underwent further purification steps, involving centrifugation and filtration through a 0.22 μm filter to exclude larger particles. Subsequently, a 3 kDa molecular filter was utilized, resulting in particles smaller than 3 kDa with a consistent size distribution, as shown in Figure 1G. All fluorescence spectra were initiated through excitation at 405 nm.

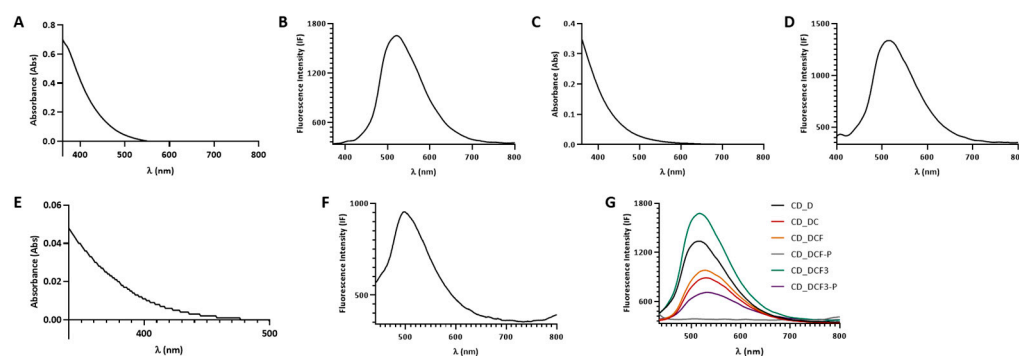


Figure 1. Optical properties of FCDs according to the absorption and emission spectra and purification processes. (A) Spectral depiction of FCDs in terms of absorbance. (B) Spectral depiction of FCDs in terms of fluorescence (B). (C,D) Absorbance and fluorescence profiles post-dialysis; (E,F) absorbance and fluorescence profiles of DEG dilution in deionized water; (G) schematic delineation of FCD purification phases. Phases/result substances: dialysis (CD_D); centrifugation (CD_DC); 0.22 μm filtration (CD_DCF) and associated pellet (CD_DCF-P); and 3 kDa filtration (CD_DCF3) and associated pellet (CD_DCF3-P).

3.2. FCD Characterization

Characterization techniques included dynamic light scattering (DLS), Fourier-transform infrared spectroscopy (FTIR) and transmission electron microscopy (TEM). DLS is able to provide valuable information about size distribution and aggregation state, alongside TEM, which, beyond size distribution and aggregation state, can also provide information about morphology, size, structure and dispersion.

In DLS, FCDs exhibited a hydrodynamic diameter below 2 nm (Figure 2A) and a zeta potential within the range of -20 to 18 mV (Figure 2B). FTIR displays the vibrational energy of covalent bonds. Each covalent bond absorbs radiation at distinct wavelengths, and so each peak in the spectrum corresponds to a functional group [18]. Figure 2C presents the transmittance spectrum of FTIR. The peak observed at $3550\text{--}3200\text{ cm}^{-1}$ is the result of O-H bonds, and further ahead in the spectrum we found more O-H bonds ($3200\text{--}2700\text{ cm}^{-1}$;

1390–1310 cm^{-1} ; 920 cm^{-1}). A double covalent bound between carbons ($\text{C}=\text{C}$) is translated into the absorption peak at 1658–1648 cm^{-1} and at 840–790 cm^{-1} . Bending vibrations from C-H bonds are observed at the absorption peak at 1450 cm^{-1} . Vibrations from C-O bonds were observed at 1275–1200 cm^{-1} and at 1085–1050 cm^{-1} . Despite the low definition of the spectrum, it is possible to induce that the FCD is a multiple hydroxyl–carbonyl compound, given the repetition of O-H groups and the presence of C=O. According to the results obtained from TEM, synthesized FCDs have a spherical morphology with a size ranging from 2 to 6 nm, with an average size of 3.1 ± 1.8 nm, illustrated in Figure 2D. Moreover, the FCD presents a crystal structure, as portrayed in Figure 2E. Despite the low zeta potential presented by FCDs, they are dispersed in an aqueous medium (Figure 2D), probably by the remaining DEG molecules, which is an unpolymerized monomer, from the reaction medium that could have been coupled to the surface layer of the nanoparticles. The expected size of these FCDs will be around 0.5, dialysis membrane tubing MWCO 100–500, and 3 kDa for the liquid filtered by centrifugation on a 3 kDa mesh.

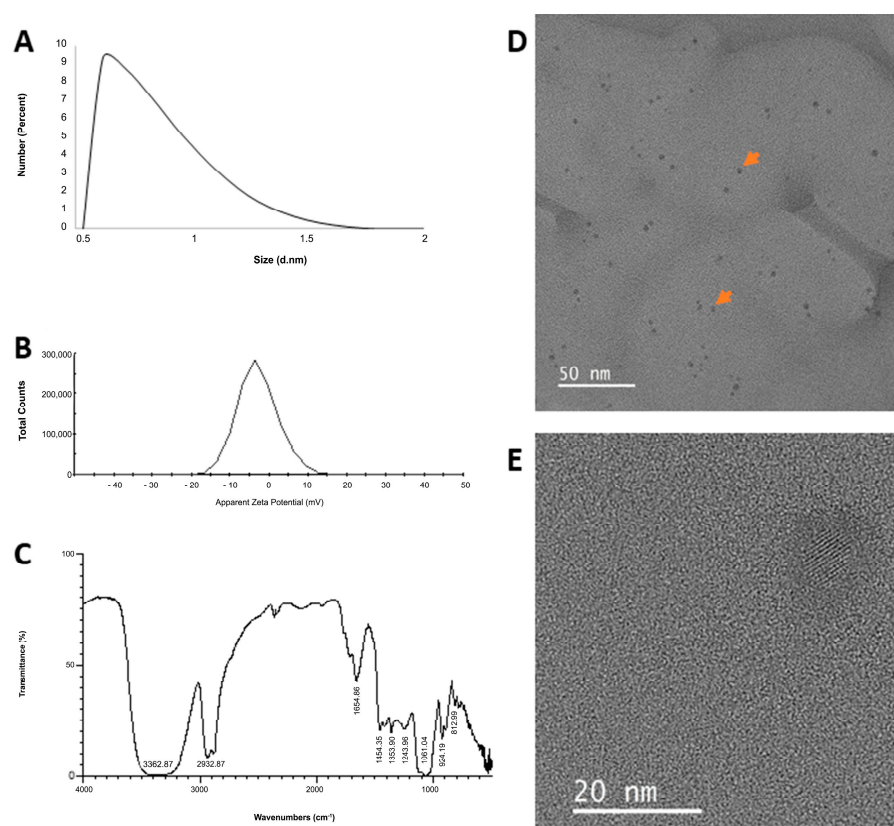


Figure 2. Characterization of FCDs according to their size, morphology, structure and functional groups. (A) Hydrodynamic diameter of FCDs; (B) zeta potential of FCDs; (C) FTIR spectrum of FCDs; (D) absorption peaks delineating specific functional groups of carbon dots: O-H, O-H, C=C, C-H, O-H, C-O, C-O, O-H, C=O, respectively. (D) Representative TEM images illustrating the size and spherical configuration of FCDs, highlighted with orange arrows; (E) high-resolution transmission electron microscopy visuals exposing their crystalline structure.

3.3. FCD Impact in Cellular Behavior

In order to establish the dose–response curve in both epithelial and tumor cell lines, we assessed the impact of FCDs on cell viability with FCD concentrations ranging from 1 mg/mL to 10 mg/mL (Figure 3). Results showed that higher FCD concentrations exhibited lower viability rates, with a more pronounced effect on the tumor cells.

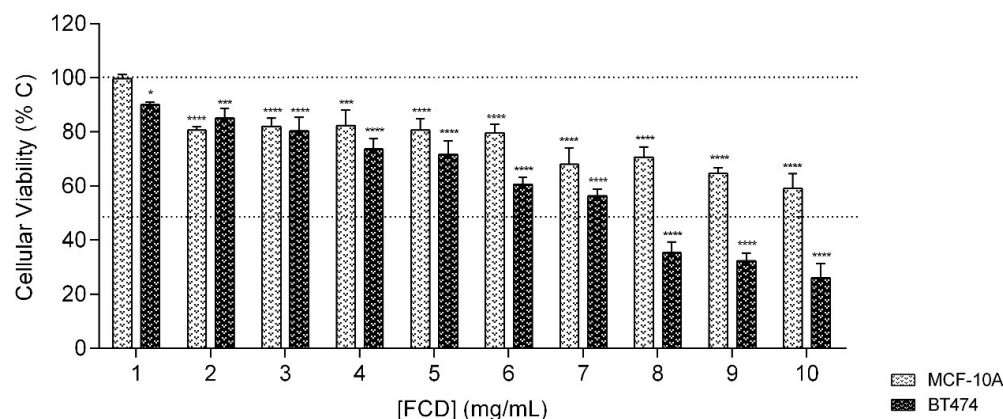


Figure 3. Effect of FCDs on breast epithelial and tumor cells assessed by cell viability. Legend: * p -value < 0.05; *** p -value < 0.001; **** p -value < 0.0001.

4. Discussion

Carbon dots have gained increasing attention in biomedicine due to their unique characteristics, which include their nanoscale size, fluorescence, low cytotoxicity, and a high integration rate into biological systems. In this study, we generated carbon dots using fructose as a novel and pioneer carbon source and investigated its potential in onco-therapeutics for breast cancer. Fructose is a glucose isomer, and its different structure results in distinct properties like high solubility and different metabolism. Previous studies found that dietary fructose intake is associated with cancer development [19], namely in breast cancer [20,21]. The study performed by Fan and colleagues observed that fructose intake was associated with increased proliferation rates in tumor cell lines, and on the other hand, fructose did not support proliferation in non-tumor cells [20]. The authors hypothesized that, since epithelial cells do not consume fructose, fructose can be specifically and selectively used as an onco-therapeutic agent.

In our study, fructose was used as a carbon source to obtain FCDs using a bottom-up method through microwave irradiation as a synthesis technique. We considered that FCDs were successfully achieved through a combination of purification methods, which included dialysis, centrifugation, filtration and lyophilization. The carbon structures were further confirmed by TEM, DLS and FTIR. TEM showcased round CDs with crystalline structures and sizes between 2 and 6 nm. DLS indicated a hydrodynamic diameter under 2 nm and a zeta potential between -20 and 18 mV. Finally, FTIR identified functional groups (O-H, C=C, C-H, C-O, C=O), characteristic of sugar-derived CDs.

Nanomedicines have demonstrated several benefits in comparison to free compounds. It was already described that nanomedicines exhibit longer blood residence time and improved drug distribution, leading to enhanced therapeutic efficacy [22]. Moreover, features like size and shape can be engineered to improve biodistribution [23], body clearance [24], and cellular uptake [25].

We used a cell-based approach to evaluate the effect of the FCDs in normal epithelial (MCF-10A) and breast tumor (BT474) cell lines and observed that FCDs exhibited higher toxicity in tumor cells. Since CDs typically exhibit antioxidant mechanisms, we evaluated the oxidative stress status but observed no significant results. We hypothesize that our findings may be linked to the specific fructose receptor GLUT5, which is overexpressed in tumor cells [26–28] and could enhance FCD uptake by recognizing fructose on its surface [26]. This leads to selective internalization of FCD through receptor-mediated endocytosis [29]. Additionally, tumor microenvironment characteristics such as vascular permeability and extracellular matrix alterations may further promote FCD accumulation in tumor tissues [30].

We acknowledge the study's limitations, particularly the high concentration of the compound used in the cell-based assays. This high concentration could be attributed to

the low number of FCDs present in the caramel-like compound after purification. Further research is necessary to better understand the impact of FCDs on normal tissues and to identify the specific pathways affected by FCDs. Additionally, exploring the functionalization of FCDs with chemotherapeutics is an intriguing prospect, as it could potentially reduce the adverse side effects of chemotherapy [31].

In conclusion, our study explored the potential of fructose-derived CDs as oncotherapeutics for breast cancer, their characterization and cellular impact. Our study lays the groundwork for future investigations, including the potential functionalization of FCDs with clinically relevant drugs and their evaluation as antitumor agents. Further research in this emerging field promises to advance our understanding of nanoparticle–cell interactions, paving the way for innovative cancer treatment approaches.

Author Contributions: Conceptualization: A.D.; Formal analysis: A.D., C.L. and S.M.; Funding acquisition: A.D. and C.L.; Investigation: S.M.; Methodology: A.D., C.L. and S.M.; Resources: A.D. and C.L.; Supervision: A.D. and C.L.; Validation: A.D. and C.L.; Writing—original draft: S.M.; Writing—review and editing: A.D., C.L. and S.M. All authors have read and agreed to the published version of the manuscript.

Funding: This research was partially supported by a scholarship awarded to Carla Luís (LPCC-NRN 2024). This work was supported by funding of the European Union (FEDER funds through Compete) and National Funds (FCT/MCTES) through Project LA/P/0008/2020 DOI 10.54499/LA/P/0008/2020, UIDP/50006/2020 DOI 10.54499/UIDP/50006/2020 and UIDB/50006/2020 DOI 10.54499/UIDB/50006/2020, UIDB/04730/2020 and UIDP/04730/2020.

Institutional Review Board Statement: Not applicable.

Informed Consent Statement: Not applicable.

Data Availability Statement: The raw data supporting the conclusions of this article will be made available by the authors on request.

Acknowledgments: The authors would like to acknowledge Raquel Soares (FMUP/i3S) for assisting in the manuscript's revision.

Conflicts of Interest: The authors declare no conflicts of interest.

References

1. Aup-Ngoen, K.K.; Noipitak, M.; Sudchanham, J.; Chiablam, C.; Kaowphong, S.; Tuantranont, A.; Srisamran, N. The impact of carbon nanoparticles derived from sucrose, glucose, and fructose precursors on the performance of fully printed perovskite solar cells. *Mater. Today Commun.* **2024**, *39*, 108549. [[CrossRef](#)]
2. Sharma, A.; Das, J. Small molecules derived carbon dots: Synthesis and applications in sensing, catalysis, imaging, and biomedicine. *J. Nanobiotechnol.* **2019**, *17*, 92. [[CrossRef](#)] [[PubMed](#)]
3. Pandey, V.K.; Tripathi, A.; Taufeeq, A.; Dar, A.H.; Samrot, A.V.; Rustagi, S.; Malik, S.; Bhattacharya, T.; Kovacs, B.; Shaikh, A.M. Significance and applications of carbon dots in anti cancerous nanodrug conjugate development: A review. *Appl. Surf. Sci. Adv.* **2024**, *19*, 100550. [[CrossRef](#)]
4. Markovic, Z.M.; Ristic, B.Z.; Arsin, K.M.; Klisic, D.G.; Harhaji-Trajkovic, L.M.; Todorovic-Markovic, B.M.; Kepic, D.P.; Kravic-Stevovic, T.K.; Jovanovic, S.P.; Milenkovic, M.M.; et al. Graphene quantum dots as autophagy-inducing photodynamic agents. *Biomaterials* **2012**, *33*, 7084–7092. [[CrossRef](#)]
5. Padidham, S.; Kandam, D.; Thakkellapati, S.C.; Verma, M.; Raichur, A.M.; Ramana, L.N.; Padidam, S.R. Single-step synthesis of self-assembled carbon dots for enhanced cancer cell retention and theranostics applications. *Microchem. J.* **2024**, *198*, 110144. [[CrossRef](#)]
6. Bhattacharya, T.; Shin, G.H.; Kim, J.T. Carbon Dots: Opportunities and Challenges in Cancer Therapy. *Pharmaceutics* **2023**, *15*, 1019. [[CrossRef](#)]
7. Deo, S.V.S.; Sharma, J.; Kumar, S. GLOBOCAN 2020 Report on Global Cancer Burden: Challenges and Opportunities for Surgical Oncologists. *Ann. Surg. Oncol.* **2022**, *29*, 6497–6500. [[CrossRef](#)]
8. Dass, S.A.; Tan, K.L.; Rajan, R.S.; Mokhtar, N.F.; Adzmi, E.R.M.; Rahman, W.F.W.A.; Din, T.A.D.A.-A.T.; Balakrishnan, V. Triple Negative Breast Cancer: A Review of Present and Future Diagnostic Modalities. *Medicina* **2021**, *57*, 62. [[CrossRef](#)] [[PubMed](#)]
9. Yersal, O.; Barutca, S. Biological subtypes of breast cancer: Prognostic and therapeutic implications. *World J. Clin. Oncol.* **2014**, *5*, 412–424. [[CrossRef](#)] [[PubMed](#)]
10. Aminolroayaei, F.; Shahbazi-Gahrouei, D.; Shahbazi-Gahrouei, S.; Rasouli, N. Recent nanotheranostics applications for cancer therapy and diagnosis: A review. *IET Nanobiotechnol.* **2021**, *15*, 247–256. [[CrossRef](#)]

11. Yang, F.; He, Q.; Dai, X.; Zhang, X.; Song, D. The potential role of nanomedicine in the treatment of breast cancer to overcome the obstacles of current therapies. *Front. Pharmacol.* **2023**, *14*, 1143102. [[CrossRef](#)] [[PubMed](#)]
12. Wei, C.; Huang, Q.; Hu, S.; Zhang, H.; Zhang, W.; Wang, Z.; Zhu, M.; Dai, P.; Huang, L. Simultaneous electrochemical determination of hydroquinone, catechol and resorcinol at Nafion/multi-walled carbon nanotubes/carbon dots/multi-walled carbon nanotubes modified glassy carbon electrode. *Electrochim. Acta* **2014**, *149*, 237–244. [[CrossRef](#)]
13. Qu, Y.; Han, B.; Yu, Y.; Yao, W.; Bose, S.; Karlan, B.Y.; Giuliano, A.E.; Cui, X. Evaluation of MCF10A as a reliable model for normal human mammary epithelial cells. *PLoS ONE* **2015**, *10*, e0131285. [[CrossRef](#)] [[PubMed](#)]
14. Holliday, D.L.; Speirs, V. Choosing the right cell line for breast cancer research. *Breast Cancer Res.* **2011**, *13*, 215. [[CrossRef](#)] [[PubMed](#)]
15. Tiron, C.E.; Luta, G.; Butura, M.; Zugun-Eloae, F.; Stan, C.S.; Coroaba, A.; Ursu, E.-L.; Stanciu, G.D.; Tiron, A. NHF-derived carbon dots: Prevalidation approach in breast cancer treatment. *Sci. Rep.* **2020**, *10*, 12662. [[CrossRef](#)]
16. Wang, Z.; Liao, H.; Wu, H.; Wang, B.; Zhao, H.; Tan, M. Fluorescent carbon dots from beer for breast cancer cell imaging and drug delivery. *Anal. Methods* **2015**, *7*, 8911–8917. [[CrossRef](#)]
17. Naik, G.G.; Alam, B.; Pandey, V.; Dubey, P.K.; Parmar, A.S.; Sahu, A.N. Pink Fluorescent Carbon Dots Derived from the Phytomedicine for Breast Cancer Cell Imaging. *ChemistrySelect* **2020**, *5*, 6954–6960. [[CrossRef](#)]
18. What is FTIR Spectroscopy? Available online: <https://www.sigmaaldrich.com/PT/en/technical-documents/technical-article/analytical-chemistry/photometry-and-reflectometry/ftir-spectroscopy> (accessed on 26 May 2023).
19. Charrez, B.; Qiao, L.; Hebbard, L. The role of fructose in metabolism and cancer. *Horm. Mol. Biol. Clin. Investig.* **2015**, *22*, 79–89. [[CrossRef](#)]
20. Fan, X.; Liu, H.; Liu, M.; Wang, Y.; Qiu, L.; Cui, Y. Increased utilization of fructose has a positive effect on the development of breast cancer. *PeerJ* **2017**, *5*, e3804. [[CrossRef](#)] [[PubMed](#)]
21. Karbassi, M.; Monzavi-Karbassi, B.; Hine, R.J.; Stanley, J.S.; Ramani, V.P.; Carcel-Trullols, J.; Whitehead, T.L.; Kelly, T.; Siegel, E.R.; Artaud, C.; et al. Fructose as a carbon source induces an aggressive phenotype in MDA-MB-468 breast tumor cells. *Int. J. Oncol.* **2010**, *37*, 615–622. [[CrossRef](#)]
22. McDonald, D.M.; Baluk, P. Significance of blood vessel leakiness in cancer. *Cancer Res.* **2002**, *62*, 5381–5385. [[PubMed](#)]
23. Perrault, S.D.; Walkey, C.; Jennings, T.; Fischer, H.C.; Chan, W.C.W. Mediating tumor targeting efficiency of nanoparticles through design. *Nano Lett.* **2009**, *9*, 1909–1915. [[CrossRef](#)] [[PubMed](#)]
24. Walkey, C.D.; Olsen, J.B.; Guo, H.; Emili, A.; Chan, W.C.W. Nanoparticle size and surface chemistry determine serum protein adsorption and macrophage uptake. *J. Am. Chem. Soc.* **2012**, *134*, 2139–2147. [[CrossRef](#)] [[PubMed](#)]
25. Jiang, W.; Kim, B.Y.S.; Rutka, J.T.; Chan, W.C.W. Nanoparticle-mediated cellular response is size-dependent. *Nat. Nanotechnol.* **2008**, *3*, 145–150. [[CrossRef](#)]
26. Zamora-León, S.P.; Golde, D.W.; I Concha, I.; I Rivas, C.; Delgado-López, F.; Baselga, J.; Nualart, F.; Vera, J.C. Expression of the fructose transporter GLUT5 in human breast cancer. *Proc. Natl. Acad. Sci. USA* **1996**, *93*, 1847–1852. [[CrossRef](#)] [[PubMed](#)]
27. Nakagawa, T.; Lanasa, M.A.; Millan, I.S.; Fini, M.; Rivard, C.J.; Sanchez-Lozada, L.G.; Andres-Hernando, A.; Tolan, D.R.; Johnson, R.J. Fructose contributes to the Warburg effect for cancer growth. *Cancer Metab.* **2020**, *8*, 16. [[CrossRef](#)] [[PubMed](#)]
28. Nahrjou, N.; Ghosh, A.; Tanasova, M. Targeting of glut5 for transporter-mediated drug-delivery is contingent upon substrate hydrophilicity. *Int. J. Mol. Sci.* **2021**, *22*, 5073. [[CrossRef](#)]
29. Oh, N.; Park, J.-H. Endocytosis and exocytosis of nanoparticles in mammalian cells. *Int. J. Nanomed.* **2014**, *9*, 51–63. [[CrossRef](#)]
30. Henke, E.; Nandigama, R.; Ergün, S. Extracellular Matrix in the Tumor Microenvironment and Its Impact on Cancer Therapy. *Front. Mol. Biosci.* **2020**, *6*, 160. [[CrossRef](#)]
31. Hoffman, A.S. The origins and evolution of ‘controlled’ drug delivery systems. *J. Control. Release* **2008**, *132*, 153–163. [[CrossRef](#)]

Disclaimer/Publisher’s Note: The statements, opinions and data contained in all publications are solely those of the individual author(s) and contributor(s) and not of MDPI and/or the editor(s). MDPI and/or the editor(s) disclaim responsibility for any injury to people or property resulting from any ideas, methods, instructions or products referred to in the content.